Journal of Nuclear Materials 377 (2008) 52–58

Contents lists available at ScienceDirect

Journal of Nuclear Materials

journal homepage: www.elsevier.com/locate/jnucmat

Low cycle fatigue of Eurofer 97

Pierre Marmy [a,*], Tomas Kruml [b]

[a] Fusion Technology-Materials, Centre de Recherches en Physique des Plasmas, École Polytechnique Fédérale de Lausanne, 5232 Villigen PSI, Switzerland
[b] Institute of Physics of Materials, Zizkova 22, 616 62 Brno, Czech Republic

A B S T R A C T

We have investigated the low cycle fatigue and creep-fatigue properties of Eurofer 97 and observed the associated microstructural changes. The *as received* structure is composed of equiaxed subgrains and a few martensite laths with a high dislocation density. Fatigue tests have been carried out in air or in high vacuum, from room temperature to 550 °C, under total strain control. It has been found that the influence of the test temperature on the fatigue endurance is not significant. The softening behaviour as a function of the imposed strain amplitude and temperature has been analysed in detail. The softening rate is independent of the imposed strain but strongly enhanced at the highest test temperature. Creep-fatigue tests were run, imposing a 500 s dwell at the maximum tensile strain of the loading cycle, at a total strain range of 0.5%, 0.8% and 1.4%, and at 150, 300 and 550 °C. The influence of the hold time is important only at the highest test temperature, under low applied strains. It was found that at the beginning of life, at the highest temperature, the softening rate with hold times is much stronger as compared to the softening rate without hold times. The amount of stress relaxed during the dwell is independent of the applied strain, at the end of life. The effect of fatigue with and without hold times up to medium temperatures on the microstructure was to lower the dislocation density and to decompose the laths and large grains into a homogeneous structure of submicron grains. At the highest test temperature, an increase of the subgrain size and carbide coarsening were observed.

© 2008 Elsevier B.V. All rights reserved.

1. Introduction

The 9–12% Cr ferritic–martensitic steels are being presently considered as main candidate materials for the first wall components of future fusion reactors and for the window of liquid metal targets of neutron sources. Recent developments in the fusion materials program are focussed on adjusting the chemical composition to achieve low activation and fast decay properties after irradiation (so called RAFM steels) as well as on the reduction of the shift of the ductile–brittle transition temperature after irradiation. The European candidate alloy presently under investigation is called the Eurofer 97.

Since fusion reactors will be run at elevated temperatures under complex loading cycles, fatigue and creep-fatigue properties are needed as a basic input for designers. Up to now, published data on the fatigue properties of Eurofer 97 and the corresponding microstructures are scarce (see for instance Refs. [1,2]). The first part of the work is an investigation of the room temperature low cycle fatigue properties, under air. Fatigue tests were then carried out in vacuum, at different temperatures, at 150, 300, 350 and 550 °C. Finally, a series of creep-fatigue tests was run at elevated temperatures, imposing a 500 s dwell at the maximum tensile strain of the loading cycle. The aim of this work was also to check the microstructures produced during the various testing conditions.

2. Experimental details

2.1. Material

The chemical composition in wt% of Eurofer 97, Heat Nr 83697, was Cr: 8.96, V: 0.2, W: 1.08, Mn: 0.47, N: 0.021, C: 0.12 and Ta: 0.14. The material was delivered in the form of 25 mm plates. The final applied heat treatment consisted in: austenitizing at 980 °C for 31 min, followed by air cooling and tempering at 760 °C for 90 min, and subsequent air cooling.

The alloy is molybdenum, nickel and niobium free, to achieve fast radio isotopes decay properties. The chromium content is around 9% to ensure a full martensitic transformation at room temperature. The Mn concentration is relatively high (0.5%) to avoid the formation of delta ferrite. Vanadium is added as a strong carbide former. Ta is present (0.14%) to reduce prior austenite grain growth.

2.2. Specimens for mechanical tests and microscopy

The cylindrical plain specimen used in the fatigue experiments is shown in Fig. 1. It has a gauge length of 6 mm and a diameter of

* Corresponding author. Tel.: +41 56 310 29 32; fax: +41 56 310 45 29.
E-mail address: pierre.marmy@psi.ch (P. Marmy).

0022-3115/$ - see front matter © 2008 Elsevier B.V. All rights reserved.
doi:10.1016/j.jnucmat.2008.02.054

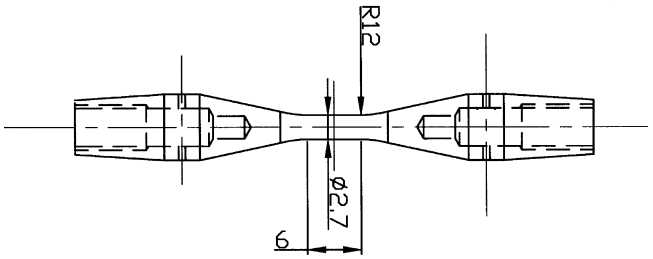

Fig. 1. Eurofer fatigue specimen.

2.7 mm. The length/diameter ratio is about 2.2 and the connecting radius is 12 mm. The chosen geometry provides stability up to high total strain ranges and at high temperatures. The specimens were machined with their longitudinal axis in the L–T orientation.

The 3 mm and 1.4 mm diameter specimens used for the transmission electron microscopy (TEM) were punched out of thin discs cut perpendicular to the specimen axis. The 1.4 mm specimens were then inserted into 3 mm stainless steel discs in order to reduce inconsistencies connected with TEM observations of magnetic specimens. The discs were thinned with a solution of 10% perchloric acid in ethanol, at −2 °C.

For optical microscopy, the surface of the *as received* material was carefully polished, then electro etched by saturated oxalic acid at room temperature and 10.5 V. The fracture surfaces were observed by scanning electron microscopy.

2.3. Testing equipment

The tests were conducted with an electro-mechanical test machine, equipped with a high vacuum furnace with a minimal pressure of 8×10^{-7} mbar. The displacement was transmitted axially by two ceramic rods connected to a sensor mechanism equipped with strain gauges in full bridge. The tests were performed under control of the total strain amplitude. Most of the testing was conducted at strain rates around $2 \times 10^{-3}\ s^{-1}$. A fine temperature transducer was welded onto the specimen gauge length for all tests. The temperature of the specimen was recorded, in order to get the complete temperature history of the experiment. This was necessary for safety reasons, since some of the creep-fatigue tests lasted more than three months.

2.4. End of life criterion

A new end of life criterion has been designed, taking into account the typical stress over cyclic evolution of FM steels. The number of cycles to failure N_f is determined according to the following graphical procedure, shown in Fig. 2:

- A mean line is drawn onto the saturation part of the stress to cycle number curve.
- This line intersects with the origin ($N = 0$) at ($\Delta\sigma = \Delta\sigma_0$).
- A parallel to this line is drawn at $\Delta\sigma = \Delta\sigma_0 - 10\%\Delta\sigma_0$.
- Its intersection with the tail of the stress to cycle number curve, defines N_f.

Using this method, the number of cycles to failure was determined precisely after the test. The machine could be stopped safely before full specimen separation occurred, using simple procedures available in the commercial software.

3. Results and discussion

3.1. As received microstructure

The microstructure was observed at several magnification levels, using light microscopy, scanning electron microscopy and transmission electron microscopy. The optical micrograph shown in Fig. 3 reveals a very dense structure with small grains. The boundaries of prior austenitic grains are decorated by carbides. Nevertheless, the size of the prior austenitic grains cannot be determined with precision, the size is estimated to be within the range of 10–15 μm.

TEM micrograph is presented in Fig. 4. Most of the structure is composed of equiaxed subgrains having a size around 0.7 μm. Elongated martensitic laths are rather rare, and their thickness was determined to be close to 0.6 μm. This is in an agreement with the value of 0.7 μm given by Sauzay et al. [3]. There exist also larger grains, up to several microns in diameter, which are not fractioned into clearly developed subgrains or cells. The dislocation density is highest in the laths and small grains. There are at least two types of precipitates: fine ones which are more or less regularly distributed in the grains and large ones found mainly on the boundaries or more commonly on the triple points. The large precipitates (about 0.3 μm in diameter) were identified as carbides with high content of Cr and W. Some Ta rich carbides having a smaller dimension (<0.1 μm) were also identified. It should be noted that the Eurofer microstructure differs from F82H and other 9–12Cr steels by much smaller dimension of the prior austenitic grains. The partition of the martensitic structure [3] inside one prior austenitic grain into packets, blocks and laths is not fully appropriate in the present

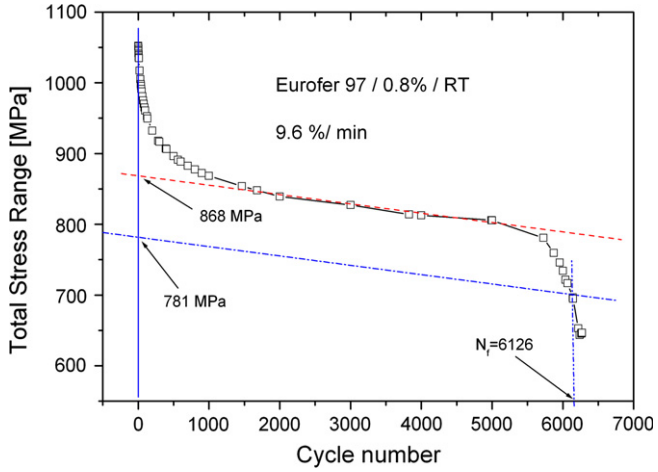

Fig. 2. Graphical method for the determination of the number of cycles to failure N_f.

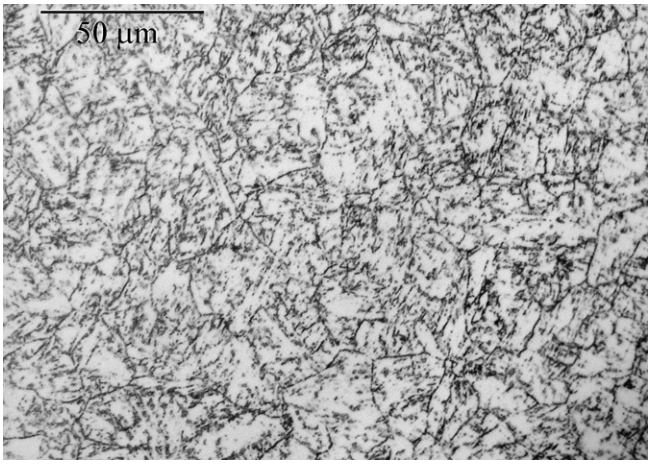

Fig. 3. Optical micrograph of Eurofer 97 showing a fine and dense structure.

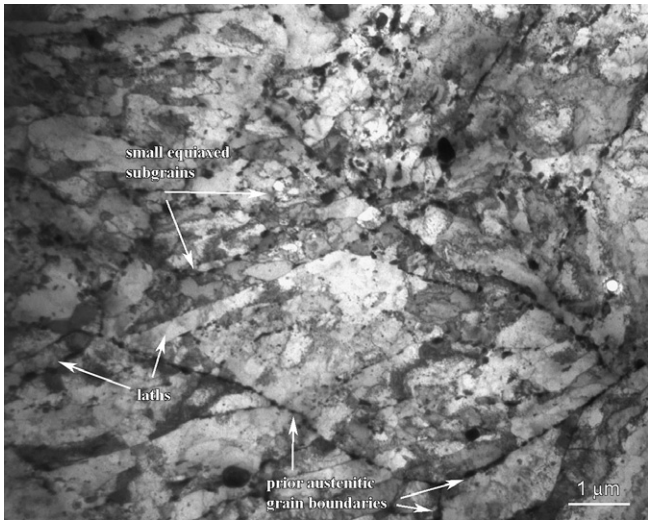

Fig. 4. Microstructure of the as received material. Prior austenitic grains are decorated by lines of carbides. Elongated martensitic laths are not frequent. The structure is composed mainly of sub micrometric equiaxed subgrains.

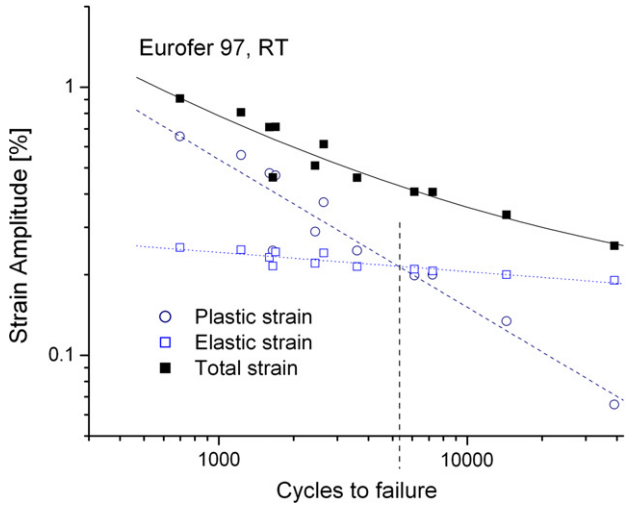

Fig. 5. Endurance of Eurofer 97 as a function of the strain amplitude, in air at room temperature.

case. At first, there is a significantly lower number of laths. The equiaxed subgrains prevail. Secondly, often a prior austenitic grain is filled by only one or two blocks of similarly oriented subgrains.

3.2. General behaviour and results at room temperature

The softening behaviour of the material corresponds to the behaviour commonly observed in ferritic–martensitic steels [4]. During the very first cycles (1–10), some little strain hardening may take place until the total stress range (the absolute difference between positive and negative stress amplitude in a cycle) shows its peak value. In most cases, the peak stress is attained in the first cycle. Only at room temperature and under low imposed strains, can this initial strain hardening phase last for a few cycles. After this very short consolidation phase, the cyclic stress amplitude decreases rapidly by about 20% of its initial level and then saturates to a value which decreases very slowly as a function of the number of cycles (see Fig. 2). This is called continuous softening since the material is continuously losing its strength. As the main crack develops in the material, a pronounced decrease of the saturation stress indicates the failure of the specimen.

The observation of the fractographs indicates that the main crack initiated always at the surface of the specimen.

The room temperature data have been evaluated according to the Coffin–Manson procedure [5,6]:

$$\Delta\varepsilon/2 = \varepsilon_a = \frac{\sigma'_f}{E}(2N_f)^b + \varepsilon'_f(2N_f)^c, \quad (1)$$

whereas, the first term, the elastic strain amplitude, is simply equal to half of the difference between the total imposed strain range and the total plastic strain range. The second term of Eq. (1) is the plastic contribution which is equal to half of the total plastic strain range. As usual, all values are taken at half life.

The total, elastic and plastic strain amplitudes of the room temperature data have been plotted in Fig. 5.

The exponent c of Eq. (1) has been calculated from the linear fit of plastic strain and is equal to $-.552$. This value is closed to the values found for similar steels, see for instance Ref. [7].

The transition life (N_f when $\Delta\varepsilon_p/2 = \Delta\varepsilon_e/2$) is around 5200 cycles.

An example of microstructure observed in a specimen fatigued at room temperature and 0.8% of strain amplitude is shown in Fig. 6. In comparison with the *as received* material, three major

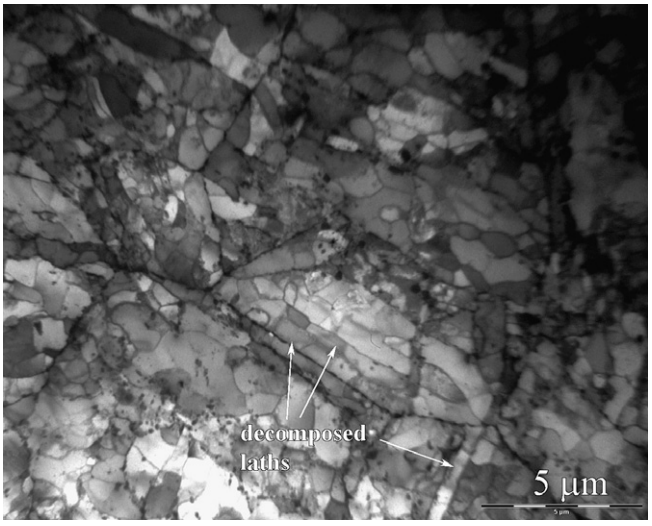

Fig. 6. Cell structure induced by the cyclic deformation in Eurofer 97, tested in air, at room temperature, at 0.8% total strain, for 7261 cycles.

microstructural modifications appear: (1) the martensitic laths are decomposed into subgrains. This evolution due to the deformation is well documented in the literature, see for instance [4]. (2) The overall dislocation density decreases. The dislocations seem to be swept out to the grain/subgrain boundaries by the cyclic plastic deformation. The grains/subgrains are, therefore, cleaner and well defined. Dislocations may be observed mainly in small grains, suspected not to be deformed plastically, or inside some grains attached and pinned by precipitates. (3) The large grains do not exist anymore. They were fractioned into fatigue cells and a quite homogeneous microstructure consisting of subgrains of around 1 micrometer in diameter is formed.

It should be noted that subgrains (i.e. grains with the misorientation comparing to their neighbors smaller than 5°, formed during the thermal treatment of the material) and fatigue cells (cells created by the dislocation activity on several crystallographic planes during the cyclic plastic deformation, resulting into small almost equiaxed volumes separated by dislocation walls having a small angle of disorientation with neighbors cells) are essentially the same objects, it is not possible to track their origin and therefore the designation of these objects is only a question of terminology.

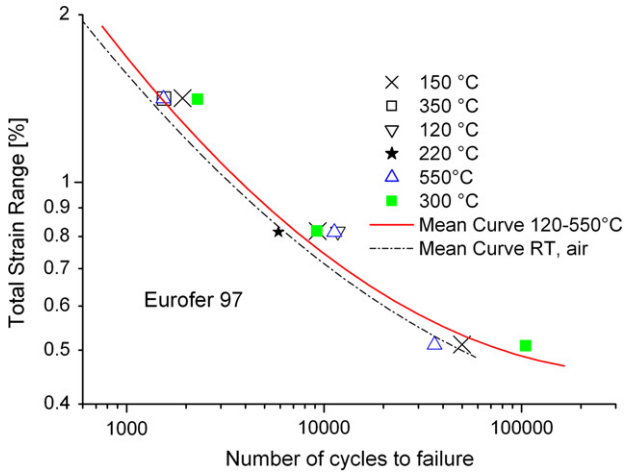

Fig. 7. Fatigue performance of Eurofer 97 at elevated temperatures, in high vacuum. The mean curve of the RT results at air is shown for comparison.

3.3. LCF at elevated temperatures

The fatigue endurance of Eurofer 97 at elevated temperatures in high vacuum is presented in Fig. 7. An influence of the temperature, if any, is not significant. For comparison, the mean curve of the data points obtained in air, at room temperature is also shown in Fig. 7. Already at room temperature, the air atmosphere seems to have a negative effect since the mean curve for RT data points is at the left hand side of the mean curve of the high temperature results.

In Fig. 8, we present the softening behaviour of the alloy, at three different temperatures, 150, 300 and 550 °C. As was reported earlier by Armas et al. [1], the final stage of the cyclic softening curve appears quasi linear in a log–log scale. Therefore, the main part of the softening curve (the last 80% of the cycles) can be described by the following equation:

$$\sigma_a = A \cdot N^{-s}, \tag{2}$$

where σ_a is the stress amplitude, A is a constant and s is the cyclic softening coefficient. Fig. 8 shows that the cyclic softening is almost identical at 150 and 300 °C, but increases significantly at 550 °C. Also interesting to note is that the cyclic softening does not depend

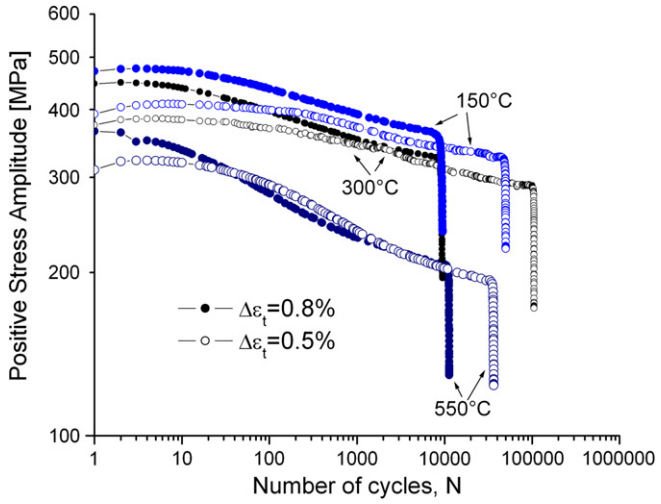

Fig. 8. Softening behaviour of Eurofer 97 at 0.8 and 0.5% total imposed strains and between 150 and 550 °C.

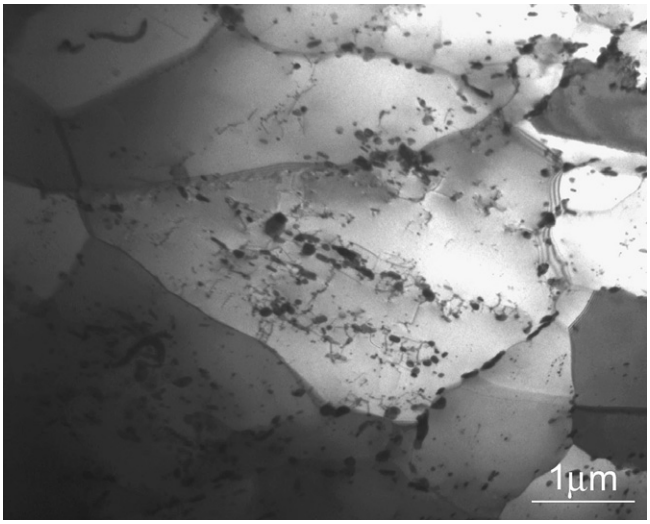

Fig. 9. Large cells observed in Eurofer 97 continuously cycled at 550 °C, in vacuum, at 0.8% total strain, for 11 273 cycles. The interior of the grain also contains isolated carbides.

on the applied strain amplitude. The larger softening observed at 550 °C is an indication for some additional softening mechanism operating at the highest temperature.

The measured softening coefficient, s, at 550 °C is 0.0485. This coefficient is close to those observed in F82H or MANET II by Armas et al. [1].

The microstructure formed at medium temperature range up to 300 °C resembles the one described for room temperature. However the highest temperature has a profound effect on the resulting microstructure. The specimen loaded at the same strain amplitude as in Fig. 6, but at 550 °C is shown in Fig. 9. It is clear that, in addition to the microstructural changes described in the previous section, a subgrain coarsening due to a coalescence of two or few neighboring subgrains, induced by cyclic deformation took place in the specimen. The submicron grains almost disappeared. The effect of the elevated temperature may be documented also by the large precipitates which are now found aligned in rows or dispersed in the interior of grains, while in the specimen deformed at room temperature they decorated grain/subgrain boundaries. Grains are almost dislocations free; no organized 3-dimensional arrangement due to fatigue process developed, as found in the ferritic steels with much larger grain sizes [8]. This observation suggests that there exists some minimal grain size which enables those regular 3D fatigue dislocation structures to be formed. While the influence of temperature on the microstructure is nicely visible in comparing Figs. 6 and 9, the plastic deformation remains the necessary condition for a rapid subgrain coarsening. This was checked by the observation of the microstructure of the undeformed heads of the same specimen (0.8% total strain amplitude, 550 °C). These heads, which were at the testing temperature but did not sustain any plastic deformation, kept the same microstructure as the *as received* material.

3.4. LCF with hold times

Seven tests have been performed, imposing a 500 s dwell at the maximum tensile strain, at RT, 150, 300 and 550 °C. Three different levels of total strain were used: high strains (1.2–1.4%) at all temperatures, medium strains (0.8%) at 300 and 550 °C and low strain (0.5%) at 550 °C.

The results are represented graphically in a classical log–log plot in Fig. 10. It can be seen that the tests run at a high imposed

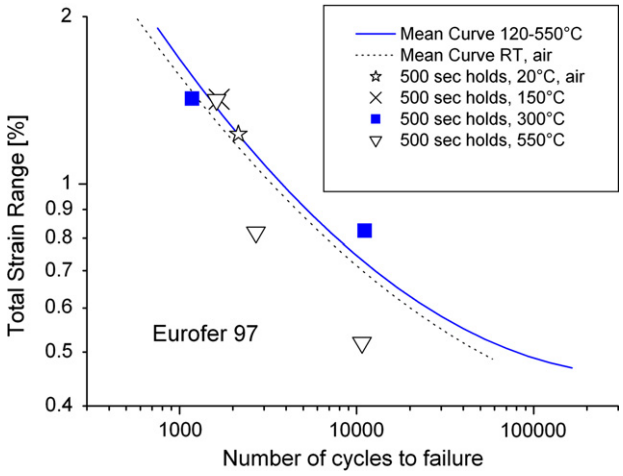

Fig. 10. Endurance plot showing the effect of 500 s tensile dwells on fatigue life.

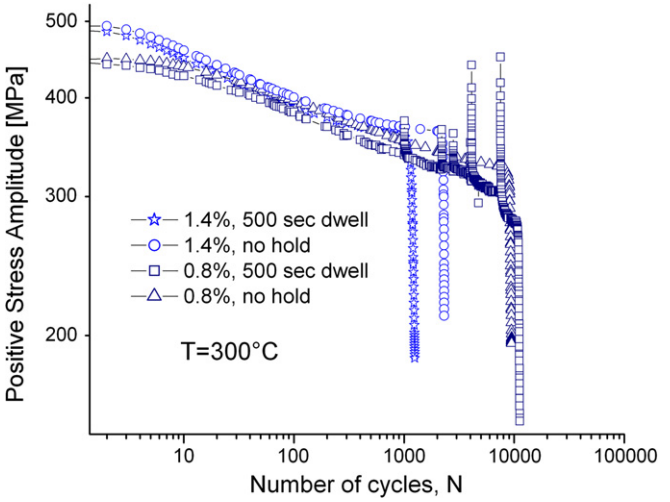

Fig. 12. Comparison of the softening behaviour with and without hold times, at 300 °C.

strain range are not strongly affected by the hold time, even at the highest test temperature. The endurance is drastically diminished at the highest test temperature, at 0.8 and 0.5% total strain. At 300 °C and 0.8% total strain, the 500 s tensile dwell has no significant effect on the fatigue life. This result is not surprising since thermal creep is not supposed to be significant at 300 °C, in ferritic–martensitic steels.

The softening behaviour at 550 °C is shown in Fig. 11, for the available tests at 0.8 and 0.5%. An interesting point to make about the diagram is that the softening rate with hold times is again independent of the applied strain but at high cycle number, seems to be lower when compared to the continuous fatigue case. Inversely, the softening rate with hold time is much stronger at the beginning of the life.

For the testing conducted with hold time, the stress level of the specimen tested at 0.5% is clearly lower than the stress level of the specimen tested at 0.8%, when compared close to end of life.

Fig. 12 shows some softening curves with and without hold times, at 300 °C. At the lower temperature the rate of softening does not seem to be very different, with or without hold times. Another important difference at 300 °C, is the much smaller difference in stress levels comparing a case with identical imposed strain, with and without an hold time. This again indicates a different material behaviour at elevated temperature, probably because of the onset of thermal creep. This is in accordance with the fact that the hold times reduce the fatigue life effectively only at 550 °C.

In Fig. 13, the relaxed stress for a 500 s hold time is shown as a function of the normalized number of cycles. Each curve represents a full test. At 550 °C, the curves for 0.5%, 0.8% and 1.4% are converging to a common value, thus indicating that the relaxed stress at end of life is independent of the imposed strain. The comparison at 0.8% and at 300 °C, indicates that at the lower temperature the relaxed stress is significantly reduced.

All curves seem to have a general behaviour very similar to the evolution of the stress range as a function of the cycles (see Fig. 2): in the first cycles the relaxed stress decreases rapidly then stabilizes to a plateau and finally drops again at end of life.

The relaxed stress appears much higher during the first cycles and this is also reflected in Fig. 11, where at the beginning of life, the softening rate at 550 °C is more important. The tensile dwell and resulting relaxation seem to be most effective during the first part of life where they efficiently accelerate the softening. At 300 °C, there is no sharp drop of the relaxed stress at beginning of life and no such effect takes place.

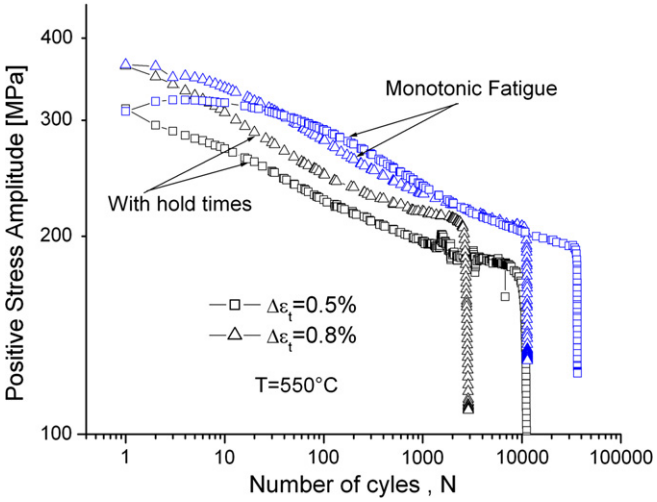

Fig. 11. Comparison of the softening behaviour with and without hold times, at 550 °C.

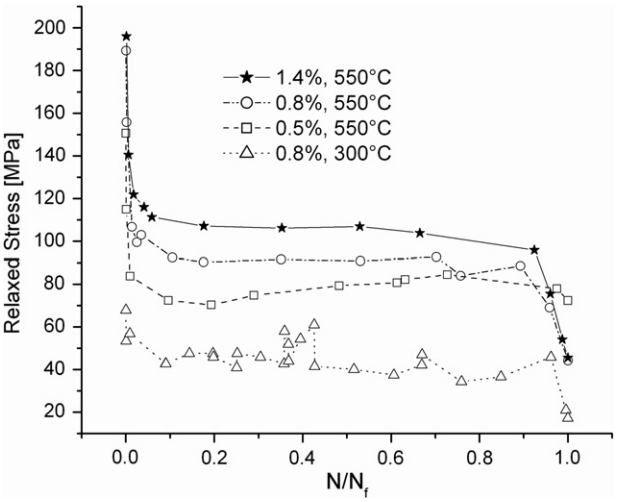

Fig. 13. Relaxed stress as a function of normalized number of cycles at different strain ranges and temperatures.

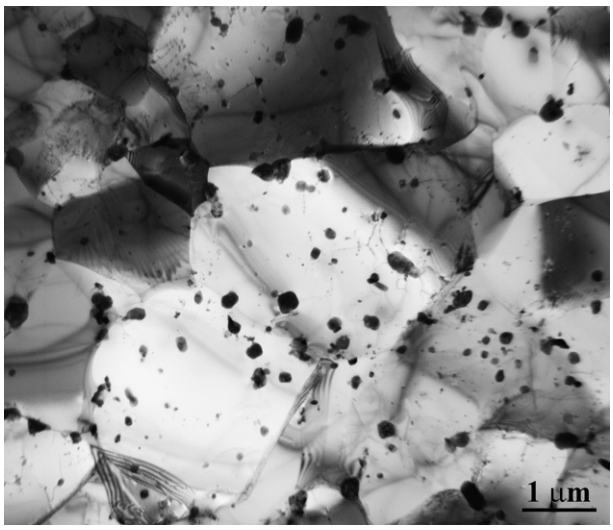

Fig. 14. Microstructure revealed by TEM in Eurofer 97 tested at 550 °C, at a total strain range of 0.5% with 500 s tensile dwells, after 10 724 cycles.

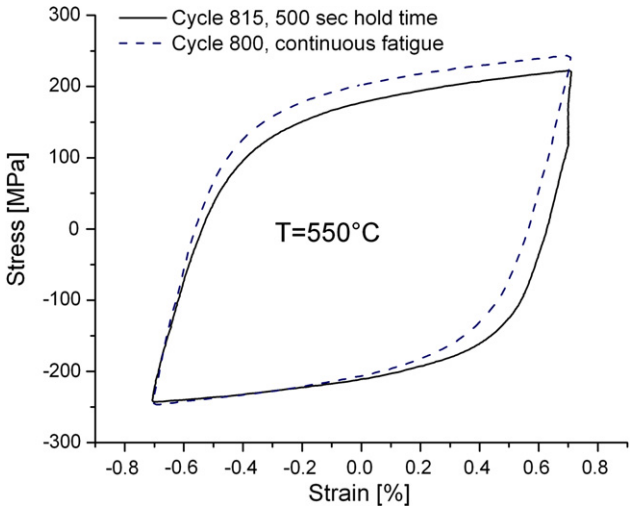

Fig. 16. Stress–strain hysteresis loops at half life of specimens tested with and without a hold time of 500 s. The specimen tested continuously has a larger flow stress. The specimen tested with hold time has a larger plastic strain. $\Delta\varepsilon_{tot} = 1.4\%$.

The microstructure (see Fig. 14) resembles the one found in the specimens tested at the same temperature in continuous fatigue (compare with Fig. 9). A qualitative analysis of the carbide morphology obtained at elevated temperatures with and without hold times indicates a clear increase of the mean carbide size when compared with the carbide morphology observed after low temperature testing (<300 °C), as observed also in [4]. It is suspected that the dwell time, which prolonged the total time of the exposure of the specimens to elevated temperature to as much as 3 months, may even induce more carbide coarsening. The statistical evaluation of carbide sizes in the observed specimens should be done to confirm this visual observation.

The evolution of the microstructure is accelerated at elevated temperatures and induces the mechanical differences described in Figs. 8, 11 and 13. These differences are mainly due to a profound modification of the microstructure: the rapid transformation of the tempered martensitic structure into large subgrains and the coarsening of the carbides.

3.5. Analysis of stress–strain hysteresis loops

Fig. 15 shows the cycle number two and the cycle at half life for a specimen with hold time tested at 550 °C and 1.4%. The cycles are not fully symmetrical, at half life the positive stress is 222.6 MPa and the negative one −243 MPa. Comparing the loops at cycle number 2 and half life, it is clear that the flow stress has decreased by a large amount and the plastic strain has increased. The amount of relaxed stress has significantly decreased, from 200 MPa at cycle number two to 103 MPa at half life. As shown in Fig. 13, the decrease of the relaxed stress occurs mainly at the beginning of life.

Fig. 16 compares the curves at half life of specimens tested with and without an hold time at 550 °C and 1.4% total imposed strain. Two obvious differences show up comparing both loops. First the specimen tested with the hold time has a lower tensile flow stress, second the same specimen has a larger plastic strain. The lower flow stress would normally lower the stress intensity factor at the crack tip, thus reducing the rate of crack propagation. On the other hand, the higher plastic flow enhances crack propagation.

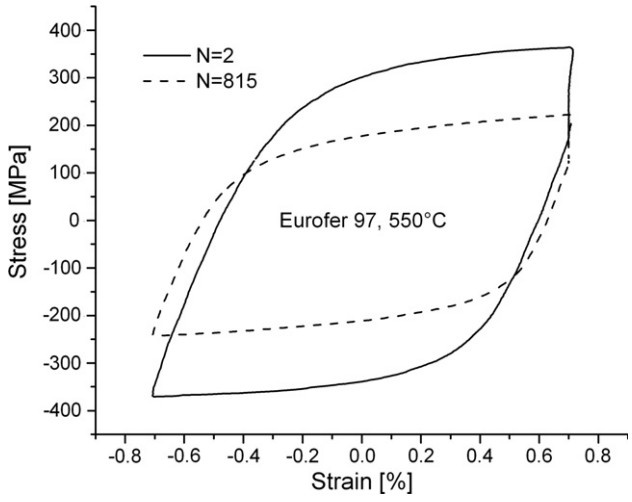

Fig. 15. Stress–strain hysteresis loops for the second and the 815th cycle (half life), at 550 °C and 1.4% total imposed strain. A dwell of 500 s is applied on the tensile stroke. The amount of relaxed stress is significantly reduced at half life.

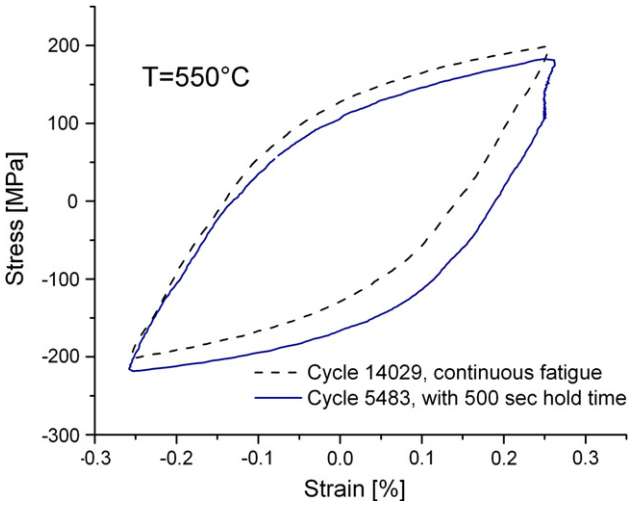

Fig. 17. Stress–strain hysteresis loops at half life of specimens tested with and without a hold time of 500 s. The specimen tested with hold time is asymmetrical and has a larger plastic strain. $\Delta\varepsilon_{tot} = 0.5\%$.

The resulting effect is surprisingly an improvement of the fatigue life (N_f = 1620 for the specimen tested with hold time and 1538 for the specimen tested without hold time). Making the same comparison at a low imposed strain range of 0.5%, as shown in Fig. 17, the situation is different because there is no visible reduction in stress (the total resulting stress range is similar) but there is a clear increase in plastic strain in the specimen with hold times. Again, the tensile dwell induces a stress asymmetry. At low imposed strains, the dwell time reduces drastically the fatigue life. The fatigue life is reduced from N_f = 36267 to N_f = 10724.

4. Conclusions

1. Eurofer 97 FM steel has been tested in air, under total strain control between 0.5% and 1.8%. The room temperature fatigue properties are similar to the ones observed in other FM steels like F82H or MANET. A tensile dwell time of 500 s has only little effect on fatigue life. The fatigue endurance at higher temperatures has been measured in high vacuum from 150 to 550 °C. There is no significant effect of test temperature on fatigue life, at the same strain amplitude. The rate of softening appears to be independent of the applied total strain. The softening rate is independent of temperature up to 300 °C, but at 550 °C it becomes much higher indicating a degradation of the structural strength of the material. The measured softening coefficient at 550 °C is similar to those measured in other FM steels.
2. At high imposed strains and at 550 °C, there is no strong influence of a 500 s hold time on fatigue life. At low imposed strains and at 550 °C, there is a strong life reduction due to the introduction of the hold time. At the beginning of life, the softening rate with hold times is much stronger as compared to the softening rate without hold times. Inversely, at the end of life, it is smaller. The amount of stress relaxed during the dwell is independent of the applied strain, close to the end of life.
3. The analysis of the stress–strain hysteresis loops has shown that the strong reduction of fatigue life observed when a tensile dwell is applied at low strains and high temperature, corresponds to a large increase of the resulting plastic strain.
4. The microstructure of the *as received* material consists mainly of equiaxed subgrains with a typical diameter of 0.6–0.7 μm and only few martensitic laths of the same width. Some large grains up to 10 μm in diameter were observed too. At least two types of carbides are present: coarse Cr and W rich carbides and fine Ta carbides. From room temperature up to 300 °C, the major changes observed in the microstructure are the decrease of the dislocation density and the decomposition of laths and large grains into a homogeneous microstructure with submicron equiaxed grains.
5. Increase of the subgrain size and carbide coarsening are the major changes qualitatively observed after high temperature cycling.

Acknowledgements

The PSI (Paul Scherrer Institute) is thanked for the technical and logistical support supplied during the testing. Financial support from the European Community Fusion Materials Program and from the research project No. AV0Z20410507 of the Academy of Sciences of the Czech Republic is gratefully acknowledged. The authors would like to thank Mrs E. Minikus for her help with preparing the microscopy specimens.

References

[1] A.F. Armas et al., J. Nucl. Mater. 329–333 (2004) 252.
[2] J. Aktaa, R. Schmitt, Fusion Eng. Des. 81 (19) (2006) 2221.
[3] M. Sauzay et al., Mater. Sci. Eng. A 400–401 (2005) 241.
[4] S. Kim, J.R. Weertman, Met. Mat. Trans. A 19A (1988) 999.
[5] L.F. Coffin, N.Y. Schenectady, Trans. ASME 76 (1954) 931.
[6] S.S. Manson, M.H. Hirschberg, in: Proceedings of the Tenth Sagamore Army Research Conference, Syracuse University, 1964.
[7] M. Victoria, et al., in: 17th Symposium on Effects of Radiation on Materials, ASTM STP 1270, Philadelphia, 1995.
[8] M. Petrenec et al., Mater. Sci. Forum 482 (2005) 179.